The Properties of Methylene- and Amine-Substituted Zeolites from First Principles

Roope Astala and Scott M. Auerbach*

Contribution from the Department of Chemistry and Department of Chemical Engineering, University of Massachusetts, Amherst, Massachusetts 01003

Received August 12, 2003; E-mail: auerbach@chem.umass.edu

Abstract: All-silica zeolite frameworks doped with methylene and amine groups are studied using density functional theory-based electron structure calculations. Strain energies are calculated in a novel way, by comparing zeolite energies with appropriate polymer reference systems. The modified zeolites are found to be mechanically stable structures with surprisingly little strain. Distortions due to impurities result in broadened Si$-$O$-$Si angle distributions in the lattice surrounding defects. Our results suggest that zeolites can accommodate both methylene and amine groups at high concentrations with minimal strain. The amine-doped zeolites are strong Lewis bases suggesting novel applications in base catalysis.

1. Introduction

Zeolites are nanoporous crystalline silicates with a wide variety of important properties and applications.[1] Recent efforts to broaden the scope of zeolite compositions have yielded LTA and MFI frameworks[2] with bridging oxygen atoms replaced by CH_2 groups.[3] Such materials may have interesting catalytic, electronic, and structural properties, which remain to be investigated. The work presented here is inspired by these experimental findings; our focus is to provide an atom- and electron-level understanding of the properties and behavior of these materials. Furthermore, we extend the scope from methylene-modified to amine-modified zeolites, to explore whether such structures are energetically feasible and chemically interesting.

CH_2 substitution is likely to produce large framework distortions, and possibly significant strain due to the atom-size mismatch and the coordination differences between carbon and oxygen atoms. It is thus surprising that CH_2-substituted zeolites can be synthesized. Indeed, the materials produced by Yamamoto et al. contain intrapore Si$-CH_3$ moieties in addition to bridging Si$-CH_2-$Si groups.[3] This raises the question whether Si$-CH_3$ groups are required to relieve strain introduced by methylene bridges. Or do methylene-substituted zeolites possess other mechanisms for relieving such strain? Furthermore, although methylene- and amine-modified zeolites involve isoelectronic substitutions, it remains interesting to explore whether these new materials exhibit novel acid$-$base properties.

In this Article, CH_2 substitutions are studied at oxygen sites in all-silica sodalite (SOD) and LTA zeolites.[2] We also model NH substitutions at oxygen sites in SOD. While $H_3SiNHSiH_3$ molecules have been studied theoretically earlier,[4] we are not aware of any prior work where the synthesis of NH doped zeolites has been considered. Therefore, it is of interest to find out whether the NH substitution is energetically possible. We investigate whether these defects are mechanically stable and provide an atomistic picture of lattice distortions near the impurities. We estimate strain energies due to these substitutions using polymer reference systems and discuss the acid$-$base properties of these materials. The modified zeolites are found to be mechanically stable structures with surprisingly little strain. Our results suggest that zeolites can accommodate both methylene and amine groups at high concentrations with minimal strain. Furthermore, the NH impurity is found to increase the Lewis base strength of an otherwise pristine sodalite.

The remainder of this Article is organized as follows: in section 2 we describe the first-principles computational methods and the model systems, in section 3 we discuss the results, and in section 4 we give concluding remarks.

2. Methods

Structures and stabilities of doped zeolites were analyzed by performing energy minimizations on materials with various doping levels. Energies were calculated using density functional theory (DFT) applied to periodic supercells using the plane-wave pseudopotential method.[5-7] The Brillouin zone was sampled using Monkhorst$-$Pack grids, and the calculations were performed within the local density approximation (LDA) of the electron exchange-correlation potential based on Ceperley$-$Alder data.[8,9] We found that the $2 \times 2 \times 2$ Monkhorst$-$Pack grid produced high enough k-point density for the results to be well converged. Electron ground states were obtained using iterative diagonalization as implemented in the VASP code.[10-13] Ion

(1) *Handbook of Zeolite Science and Technology*; Auerbach, S. M., Carrado, K. A., Dutta, P. K., Eds.; Marcel Dekker: New York, 2003.
(2) Baerlocher, C.; Meier, W. M.; Olson, D. H. *Atlas of Zeolite Framework Types*, 5th ed.; Elsevier: Amsterdam, 2001.
(3) Yamamoto, K.; Sakata, Y.; Nohara, Y.; Takahashi, Y.; Tatsumi, T. *Science* **2003**, *300*, 470.
(4) Tossell, J. A.; Gibbs, G. V. *Acta Crystallogr.* **1978**, *A34*, 463.
(5) Hohenberg, P.; Kohn, W. *Phys. Rev.* **1964**, *136*, B864$-$B871.
(6) Kohn, W.; Sham, L. *Phys. Rev.* **1965**, *140*, A1133$-$A1138.
(7) Payne, M. C.; Teter, M. P.; Allan, D. C.; Arias, T. A.; Joannopoulos, J. D. *Rev. Mod. Phys.* **1992**, *64*, 1045$-$1097.
(8) Monkhorst, H. J.; Pack, J. D. *Phys. Rev. B* **1974**, *13*, 5188$-$5192.
(9) Ceperley, D. M.; Alder, B. J. *Phys. Rev. Lett.* **1980**, *45*, 566$-$569.
(10) Vienna Ab Initio Software Package, developed at Institüt für Materialphysik, Universität Vienna.
(11) Kresse, G.; Hafner, J. *Phys. Rev. B* **1993**, *45*, 558.
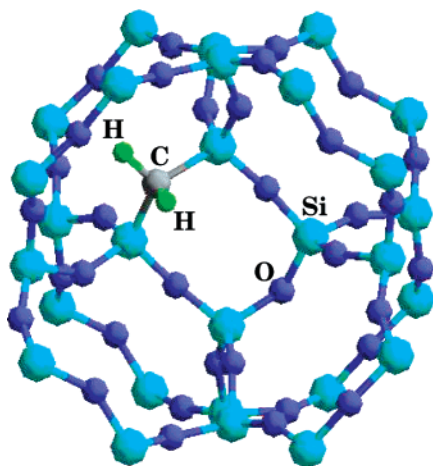
Figure 1. The sodalite cage with a CH$_2$ impurity substituting a bridging oxygen, relaxed structure.

cores were represented by Vanderbilt-type ultrasoft pseudopotentials provided within the VASP package.[14,15] In these potentials, the orbitals (3s, 3p) on Al and Si; (2s, 2p) on B, C, N, O, and F; and (1s) on H are included in the set of explicitly treated valence states. In practice, we found excellent convergence using a plane-wave cutoff of 420 eV. This DFT-LDA method has been shown to accurately reproduce framework geometries and lattice parameters of various silica polymorphs when compared to experimental data, and also to DFT calculations using the gradient-corrected Perdew–Wang (PW91) functional.[16] These methods have been applied previously to study other phenomena in zeolites. A noncomprehensive list includes chemisorption in chabazite,[17] structural properties of all-silica and acidic mordenite bulk crystals and surfaces,[18,19] and reaction mechanisms in zeolites.[20]

CH$_2$ and NH impurities were introduced by replacing bridging oxygens in silica sodalite (SOD). The SOD framework containing one CH$_2$ impurity is shown in Figure 1. This framework was chosen because of its relatively simple unit cell (cubic, Si$_{12}$O$_{24}$)[2], and because SOD is one of the building units of LTA zeolite in which CH$_2$ doping was experimentally realized.[3] To obtain defect concentrations similar to those reported in ref 3, 1–3 CH$_2$ or NH substitutions were incorporated per unit cell. In addition, the behavior at much higher defect concentrations was investigated by substituting half or 12 oxygens, and all 24 oxygens with CH$_2$ groups.

A variety of energy minimizations were performed to gauge mechanical stability. We began by optimizing the lattice parameter and internal coordinates of pristine silica SOD, henceforth denoted as OXY-SOD. The space group of OXY-SOD was constrained to that of the low-symmetry $I\bar{4}3m$ phase.[21] The doped sodalites are denoted nCH$_2$–SOD and nNH–SOD, where n is the number of dopants per SOD unit cell. For each doped sodalite, internal (i) and full (f) minimizations were performed. In (i) minimizations, atomic positions were allowed to relax, while the lattice parameter a was fixed to the calculated OXY-

SOD value of 8.83 Å. These geometry optimizations were performed using the conjugate gradients algorithm.[22] In (f) minimizations, which probe the effect of doping on unit cell volume, the energy is optimized with respect to both the lattice parameter and the atomic coordinates. With the doped structures, no symmetry constraint was imposed on the atoms, apart from keeping the unit cell shape cubic.

The CH$_2$ impurity in all-silica LTA was studied as well. The LTA framework type also has a cubic unit cell, with composition Si$_{24}$O$_{48}$.[2] As with OXY-SOD, a pristine OXY-LTA unit cell was first relaxed with respect to its lattice parameter and atomic positions. The OXY-LTA framework contains three crystallographically distinct oxygens which we denote as O(a), O(b), and O(c). These differ mainly in their Si–O–Si angles: Θ(a) = 146.7°, Θ(b) = 150.0°, and Θ(c) = 156.5°. A single CH$_2$ substitution on each of these sites was examined, denoted CH$_2$-LTA(α) where α = a, b, or c. Only internal (i) minimizations of CH$_2$-LTA(α) were performed due to the computer-intensive nature of the calculations. This approximation is justified by our calculations on doped sodalites, which show that unit cell volume relaxation is negligible at such low defect concentrations. The space group of OXY-LTA was constrained to $Pm\bar{3}m$,[2] while the doped LTA structures were relaxed without constraints.

Although the total energy of doped SOD and LTA zeolites is straightforward to calculate using the methods outlined above, estimating the strain energy in these systems is less straightforward. This is because the energy difference between, for example, OXY-SOD and nCH$_2$-SOD involves contributions from both chemical substitution and lattice strain. The chemical substitution energy is uninteresting because the silica source used by Yamamoto et al. already contains Si–CH$_2$–Si groups.[3] We proceed to evaluate the strain energy, denoted E^s, by comparing with suitable reference systems that have minimal strain in the sense that bond lengths and angles are free to relax without network constraints.

Silica chain polymers were chosen as reference systems. These include all-silica (SiO)$_2$(OH)$_4$ and doped (SiNH)(SiO)(OH)$_4$ and (SiCH$_2$)(SiO)(OH)$_4$ polymers (see Figure 2). Each doped polymer contains an impurity in a chemical environment analogous to that in the doped zeolites. The chains are periodic in the x-direction and are separated from their periodic replicas in y- and z-directions by a large vacuum region. The energy of each polymer is minimized with respect to both internal coordinates and supercell repeat length, hence releasing all possible strain. As such, we estimate the defect strain energy (per defect) for nCH$_2$–SOD as:

$$E^s_{n\mathrm{CH}_2-\mathrm{SOD}} = n^{-1}[E_{n\mathrm{CH}_2-\mathrm{SOD}} - E_{\mathrm{OXY-SOD}}] - [E_{\mathrm{CH}_2-\mathrm{POLY}} - E_{\mathrm{OXY-POLY}}] \quad (1)$$

where $E_{n\mathrm{CH}_2-\mathrm{SOD}}$, $E_{\mathrm{OXY-SOD}}$, $E_{\mathrm{CH}_2-\mathrm{POLY}}$, and $E_{\mathrm{OXY-POLY}}$ are the energies of doped and undoped sodalites and polymers, respectively. The first term in square brackets in eq 1 is the total substitution energy per defect, containing both chemical and strain contributions. The second term in square brackets includes only the chemical substitution energy, thus leaving only strain energy in $E^s_{n\mathrm{CH}_2-\mathrm{SOD}}$. We note that $E^s_{n\mathrm{CH}_2-\mathrm{SOD}}$ is also the reaction energy per impurity for the process:

$$\mathrm{OXY\text{-}SOD} + n(\mathrm{CH}_2\text{-}\mathrm{POLY}) \rightarrow n\mathrm{CH}_2\text{-}\mathrm{SOD} + n(\mathrm{OXY\text{-}POLY})$$
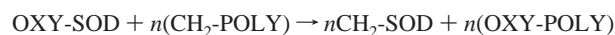
Defect strain energies for NH-doped sodalites and CH$_2$-doped LTA structures are similarly defined.

As a brief aside, we suggest that this polymer method provides a useful way to estimate an optimal Si–O–Si angle independent of network constraints, and without artifacts from hydrogen bonding. Such an Si–O–Si angle is an important input to many force field models of silica.[23] However, this parameter is difficult to extract from experimental

(12) Kresse, G.; Hafner, J. *Phys. Rev. B* **1994**, *49*, 14251.
(13) Kresse, G.; Furthmüller, J. *Phys. Rev. B* **1996**, *54*, 11169–11186.
(14) Vanderbilt, D. *Phys. Rev. B* **1990**, *41*, 7892–7895.
(15) Kresse, G.; Hafner, J. *J. Phys.: Condens. Matter* **1994**, *6*, 8245.
(16) Demuth, Th.; Jeanvoine, Y.; Hafner, J.; Ángyán, J. G. *J. Phys.: Condens. Matter* **1999**, *11*, 3833.
(17) Rozanska, X.; Demuth, T.; Hutschka, F.; Hafner, J.; van Santen, R. A. *J. Phys. Chem. B* **2002**, *106*, 3238.
(18) Demuth, T.; Hafner, J.; Benco, L.; Toulhoat, H. *J. Phys. Chem. B* **2000**, *104*, 4593.
(19) Bucko, T.; Benco, L.; Demuth, Th.; Hafner, J. *J. Chem. Phys.* **2002**, *117*, 7295.
(20) Rozanska, X.; van Santen, R. A. In *Handbook of Zeolite Science and Technology*; Auerbach, S. M., Carrado, K. A., Dutta, P. K., Eds.; Marcel Dekker: New York, 2003; p 785.
(21) Knorr, K.; Braunbarth, C. M.; van de Goor, G.; Behrens, P.; Griewatsch, C.; Depmeier, W. *Solid State Commun.* **2000**, *11*, 503.
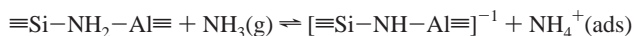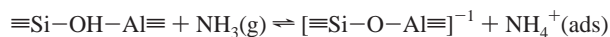
(22) Bazaraa, M. S.; Sherali, H. D.; Shetty, C. M. *Nonlinear Programming: Theory and Algorithms*; John Wiley & Sons: New York, 1993.
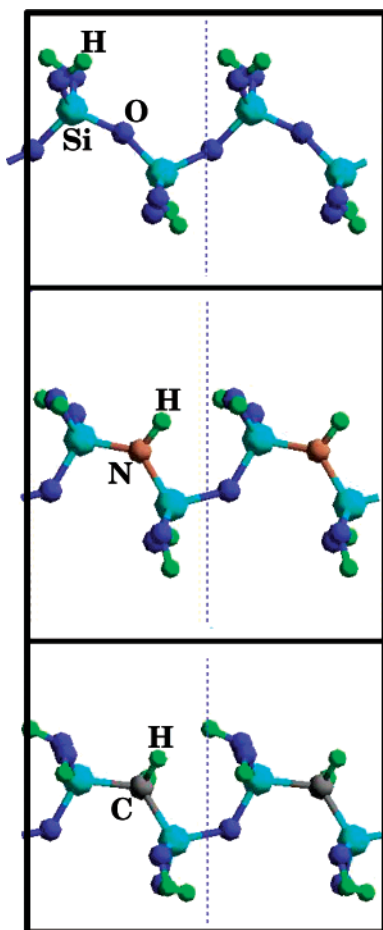
Figure 2. The three relaxed chain polymers used as reference systems. From top to bottom: $(SiO)_2(OH)_4$, $(SiNH)(SiO)(OH)_4$, and $(SiCH_2)(SiO)$-$(OH)_4$. Two repeat lengths of each polymer are shown.

structural data, which find Si−O−Si angles across the range 140−180° depending upon the particular silica polymorph.[24] Moreover, attempts to optimize this bond angle in cluster calculations are complicated by termination effects from hydrogen bonding species such as −Si(OH)₃ groups. This polymer method removes such artifacts and thus may be useful for parametrizing models of silica and other network-forming systems.

To gauge the acid−base properties of amine-doped sodalites, we calculated energies of acid−base reactions for comparison with conventional zeolites. To probe acidity, which is crucial for initiating many petrochemical processes,[25] we compared the reaction energies for the following processes:
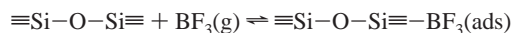
$$\equiv Si-OH-Al\equiv + NH_3(g) \rightleftharpoons [\equiv Si-O-Al\equiv]^{-1} + NH_4^+(ads)$$

$$\equiv Si-NH_2-Al\equiv + NH_3(g) \rightleftharpoons [\equiv Si-NH-Al\equiv]^{-1} + NH_4^+(ads)$$

where in both cases the process was modeled in sodalite with a single Brønsted acid site. Also, in both cases, the reactant NH_3 was isolated from the zeolite, while the product NH_4^+ was complexed through ion-pair formation with the zeolite conjugate base. As such, these reaction energies reflect heats of ammonia sorption in these materials at 0 K. Although it would be preferable to compare the intrinsic acidities of $\equiv Si-OH-Al\equiv$ and $\equiv Si-NH_2-Al\equiv$, such calculations are extremely

Table 1. Optimal Three-Body Angles and Repeat Lengths for Various Chain Polymer Structures

polymer and angle	Θ (deg)	length (Å)
CH_2CH_2		2.5
C−C−C	113.9	
H−C−H	105.2	
$CH_2SiH_2CH_2SiH_2$		6.2
C−Si−C	113.1, 113.2	
Si−C−Si	113.1, 113.2	
H−C−H	107.1	
H−Si−H	107.3	
$(SiO)_2(OH)_4$		4.9
Si−O−Si	154.1, 157.6	
$(SiNH)(SiO)(OH)_4$		5.1
Si−N−Si	129.7	
Si−O−Si	134.6	
$(SiCH_2)(SiO)(OH)_4$		5.1
Si−C−Si	123.7	
Si−O−Si	130.5	

inconvenient using periodic supercells because they require expensive corrections for charge-balancing artifacts. Comparing the energies from the reactions above still provides a good qualitative gauge of acid strength in amine-doped aluminosilicates.

Many catalytic applications such as partial oxidation[26] and halogen elimination[27] exploit zeolites as Lewis bases, that is, donors of electron density. Here, we might expect an amine-doped zeolite to be more basic than a conventional zeolite. To investigate this, we calculated BF_3 sorption energies in OXY-SOD and NH-SOD as shown below:

$$\equiv Si-O-Si\equiv + BF_3(g) \rightleftharpoons \equiv Si-O-Si\equiv -BF_3(ads)$$

$$\equiv Si-NH-Si\equiv + BF_3(g) \rightleftharpoons \equiv Si-NH-Si\equiv -BF_3(ads)$$

where $\equiv Si-X-Si\equiv -BF_3$ signifies the formation of a weak X−B bond involving lone-pair electrons on X. For all of the acid−base reactions discussed above, we first performed (i) optimizations of the bare zeolites and isolated guest molecules, using lattice parameters obtained from (f) optimizations of OXY-SOD and NH-SOD. We then performed (i) optimizations of the zeolite−guest complexes. Each of these acid−base reactions was found to be essentially barrierless, so no special coordinate-driving approach was needed to coax the zeolite−guest complexes into geometry optimization.

3. Results and Discussion

Here, we discuss the results of our calculations on chain polymers, on doped-zeolite structures and stabilities, and on acid−base properties of amine-doped sodalites.

To benchmark the reliability of the polymer models, we optimized polyethylene [PE = $(CH_2CH_2)_n$] and $(CH_2SiH_2CH_2$-$SiH_2)_n$ for comparison with experiment and with the more complex polymers. The results of all our polymer optimizations are summarized in Table 1. The DFT-LDA method predicts a C−C−C angle in PE of 113.9°, in very good agreement with earlier theoretical and experimental results (ref 28 and citations therein). The DFT-LDA method predicts that the four C−Si−C and Si−C−Si angles in $(CH_2SiH_2CH_2SiH_2)_n$ fall in the range 113.1−113.2°, suggesting that 113−114° is characteristic of carbon and silicon chains without relatively electronegative atoms such as oxygen. The two Si−O−Si angles in $((SiO)_2$-

(23) Vashishta, P.; Kalia, R. K.; Rino, J. P.; Ebbsjö, I. *Phys. Rev. B* **1990**, *41*, 12197.
(24) Wyckoff, R. W. G. *Crystal Structures*, 2nd ed.; John Wiley & Sons: New York, 1965; Vol. 1.
(25) Corma, A. *Chem. Rev.* **1995**, *95*, 559.

(26) Luo, L.; Labinger, J. A.; Davis, M. E. *J. Catal.* **2001**, *200*, 222.
(27) Murray, D. K.; Howard, T.; Goguen, P. W.; Krawientz, T. R.; Haw, J. F. *J. Am. Chem. Soc.* **1994**, *116*, 6354.
(28) Miao, M. S.; Zhang, M.-L.; Van Dore, W. E.; Van Alsenoy, G.; Martins, J. L. *J. Chem. Phys.* **2001**, *115*, 11317.

Table 2. Details of Atom-Level Geometries of Pristine and Doped Sodalites[a]

	a (Å)		Θ(Si–O–Si) (deg)
OXY-SOD	8.83 ± 0.03		156.7
OXY-LTA	11.82 ± 0.04		146.7−156.5

	a (Å)	Θ(Si–C–Si) (deg)	Θ(Si–O–Si) (deg)
CH$_2$-SOD (i)	8.83 ± 0.03	126.1	147.7−162.9
CH$_2$-SOD (f)	8.72 ± 0.03	119.1	144.8−171.4
2CH$_2$-SOD (i)	8.83 ± 0.03	126.6, 126.7	149.4−157.0
2CH$_2$-SOD (f)	8.72 ± 0.03	122.7, 122.8	146.5−156.7
3CH$_2$-SOD (i)	8.83 ± 0.03	125.3−129.5	143.6−170.9
3CH$_2$-SOD (f)	8.71 ± 0.03	121.6−126.4	142.0−172.3
12CH$_2$-SOD (i)	8.83 ± 0.03	127.3−127.7	132.3−132.7
12CH$_2$-SOD (f)	9.02 ± 0.03	130.7−130.9	137.4−137.6
24CH$_2$-SOD (i)	8.83 ± 0.03	116	
24CH$_2$-SOD (f)	9.40 ± 0.03	117.3−138.4	

	a (Å)	Θ(Si–N–Si) (deg)	Θ(Si–O–Si) (deg)
NH-SOD (i)	8.83 ± 0.03	135.5	150.1−162.2
NH-SOD (f)	8.80 ± 0.03	133.2	149.4−163.7
2NH-SOD (i)	8.83 ± 0.03	135.1, 137.5	151.2−160.1
2NH-SOD (f)	8.78 ± 0.03	133.5, 134.5	150.3−158.4
3NH-SOD (i)	8.83 ± 0.03	133.5−138.7	144.1−174.4
3NH-SOD (f)	8.72 ± 0.03	128.5−137.4	138.5−167.8

	a (Å)	Θ(Si–C–Si) (deg)	Θ(Si–O–Si) (deg)
CH$_2$-LTA (i), (a)	11.82 ± 0.04	123.9	145.7−151.4
CH$_2$-LTA (i), (b)	11.82 ± 0.04	119.0	155.4−178.1
CH$_2$-LTA (i), (c)	11.82 ± 0.04	128.9	141.9−166.1

[a] (i) denotes structures where internal coordinates were relaxed while lattice parameter a is fixed; (f) denotes structures where the lattice parameter is also relaxed. (a), (b), and (c) denote three inequivalent substitution sites in LTA framework. The values of a, as well as Si−C−Si, Si−N−Si, and Si−O−Si angles are shown. With doped structures, Si−O−Si angles of triplets neighboring the impurities are given.

(OH)$_4$)$_n$ optimize to 154.1° and 157.6°, values surprisingly larger than the ca. 145° found in most dense polymorphs of silica,[24] and assumed in some force fields parametrized for silica.[23] The Si−C−Si and Si−N−Si angles in the corresponding doped polymers optimize to 123.7° and 129.7°, respectively, suggesting that the Si−X−Si angle increases with the electronegativity of X = C, N, and O, although not linearly. These Si−X−Si angles are quite a bit larger than one would naively expect from standard sp^3 hybridization arguments. One possible explanation for this finding is that pendant −OH groups polarize Si atoms giving them partial positive charges, producing electrostatic repulsions between silicons that are reduced with increased Si−X−Si angles. For all three silica chain polymers, pendant −OH groups were found to be sufficiently far from one another to make hydrogen bonding negligible.

In all cases, the doped sodalites were found to be stable in the sense that no bond-breaking was observed upon relaxation. Structural parameters for pure and doped SOD and LTA zeolites are summarized in Table 2. The lattice parameter for OXY-SOD of a = 8.83 Å falls to 8.72 Å for CH$_2$-SOD (1.3% decrease) and remains close to that value for 2 and 3 defects per SOD unit cell. Alternatively, the lattice parameter for nNH−SOD falls monotonically to 8.72 Å from 1 to 3 defects per unit cell. These defects (at low concentrations) shrink the lattice parameter because the Si−C−Si and Si−N−Si angles in doped sodalites are substantially smaller than the corresponding Si−O−Si angle in OXY-SOD. These angles tend to decrease when relaxing the lattice parameter a, but generally remain in the range 120−130° for Si−C−Si and 130−140° for
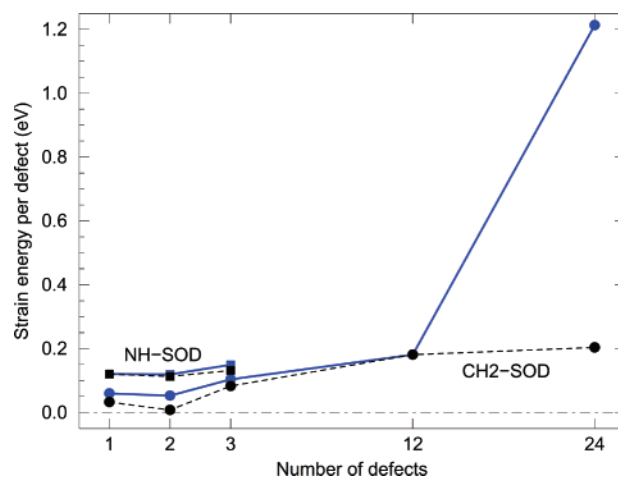
Figure 3. The defect strain energies E^s per impurity for doped sodalite systems. Circles denote CH$_2$ doped systems, and squares denote NH doped ones. Black dashed lines denote systems where the lattice parameter is relaxed, while the blue lines denote systems where the parameter is fixed.

Si−N−Si. The fact that these angular ranges overlap those found from the polymer calculations foreshadows the possibility that these doped sodalites exhibit little strain. For 12 and 24 CH$_2$ defects per unit cell, the lattice parameter actually increases to 9.02 and 9.40 Å (6.5% increase), respectively, largely because of increasing Si−C bond lengths (more on that below). In ref 3, a lattice parameter expansion of 0.1−0.2% was observed for 1 wt % CH$_2$-doped MFI, as compared to silicalite-1. Thus, the effect of low-to-moderate doping on the lattice parameters is likely to be small.

Strain due to impurity substitutions results in distortions of Si−O−Si angles near defects as shown in Table 2. For example, the Si−O−Si angle of 156.7° in OXY-SOD broadens to 142−172° in 3CH$_2$-SOD. These distortions are slightly less pronounced for nNH-SOD than for nCH$_2$-SOD. In contrast, Si−O bond lengths in doped sodalites take values nearly unchanged from the 1.59 Å found in OXY-SOD. With 1−3 defects, Si−C and Si−N bond lengths take values of 1.80−1.83 and 1.68−1.70 Å, respectively. In the half- and fully doped structures, Si−C bond lengths increase to 1.83−1.84 and 1.84−1.91 Å, respectively. These Si−C bond lengths found in 24CH$_2$−SOD are characteristic of bonding in silicon carbide. In particular, applying the same DFT-LDA approach to silicon carbide yields an Si−C bond length of 1.88 Å, which is consistent with previous results (1.86−1.87 Å) obtained using DFT-LDA with norm-conserving pseudopotentials.[29]

Our results show that distorting Si−O−Si angles is the main stress-relief mechanism in doped SOD and LTA zeolites. In contrast, X−Si−O distortions are found to be relatively small. For example, while O−Si−O angles in OXY-SOD are nearly tetrahedral, C−Si−O angles in 3CH$_2$−SOD fall in the range 105−118°. Only in the fully doped 24CH$_2$−SOD system do we find significant distortion of C−Si−C angles, taking values from 97° to 123° in the fully relaxed structure. While our structural data clearly show that distorting Si−O−Si angles provides the lowest-energy route to minimizing strain, the question remains how much residual strain exists in these materials.

The strain energy per defect, E^s, is shown in Figure 3 for doped sodalites. Strain energies are found to be as small as 0.10

(29) Käckell, P.; Wenzien, B.; Bechstedt, F. *Phys. Rev. B* **1994**, *50*, 17037.

Table 3. Interatomic Distances at Si−NH₂-Si, Si−OH−Al, and Si−O−Si Sites after Adsorption of NH₃ or BF₃[a]

NH₃ + Si−NH₂−Al	$d(N_f-H) = 1.12$ Å	$d(H-N_m) = 1.58$ Å
NH₃ + Si−OH−Al	$d(O_f-H) = 1.48$ Å	$d(H-N_m) = 1.10$ Å
BF₃ + Si−O−Si	$d(O_f-B) = 1.71$ Å	
BF₃ + Si−NH−Si	$d(N_f-B) = 1.67$ Å	

[a] N_f and O_f refer to the framework N and O, while N_m refers to the guest molecule N. Distances for the reacting H are shown.

**Table 4.** Adsorption Energies of NH₃ and BF₃ at Various Sites

	adsorption energy (eV)
NH₃ + Si−NH₂−Al	−0.9
NH₃ + Si−OH−Al	−1.7
BF₃ + Si−O−Si	−0.5
BF₃ + Si−NH−Si	−0.8

Figure 4. The density of Kohn−Sham eigenstates for singly doped and pristine sodalites. The internal coordinates and lattice parameter are relaxed. The Fermi energy E_F has been scaled to zero.

eV for nCH₂-SOD and 0.15 eV for nNH-SOD. The strain energy per CH₂ impurity increases at higher doping concentrations as shown in Figure 3. In fully CH₂-doped SOD, the strain energy per defect is significantly larger, 1.21 eV, before relaxing the lattice parameter, but it decreases to 0.20 eV after full relaxation. In CH₂-doped LTA, the defect strain energy takes values of nearly zero for the (a) site and 0.14 eV for the (b) and (c) sites, indicating that the ability of the lattice to accommodate defects can vary from site to site.

These surprisingly small strain energies arise because of the remarkable ability of silicate materials to adopt a broad range of Si−O−Si angles with little to no energetic cost. This fact, which remains poorly understood at the electronic structure level, underlies the structural versatility of zeolites in particular and silicates in general. Our results show that the Si−CH₃ groups found in the materials synthesized by Yamamoto et al.[3] may not be required to relieve strain, suggesting that synthesizing analogous materials without Si−CH₃ groups should be thermodynamically possible.

Having now described the structure and stability of amine-doped zeolites, we now turn to their properties as adsorbents. Adsorption energies of NH₃ at Si−NH₂−Al and Si−OH−Al sites in SOD are shown in Table 4. The NH₃ adsorption energy at the Si−OH−Al site predicted by DFT-LDA is −1.7 eV, in reasonable agreement with experimental heats of NH₃ adsorption which fall in the range 1.1−1.7 eV for low NH₃ loading in various high silica zeolites.[30] NH₃ adsorption at the Si−OH−Al site involves ion-pair formation between NH₄ and Si−O−Al. On the other hand, NH₃ adsorption at the Si−NH₂−Al site does not involve such ion-pair formation; instead, we find simple physisorption with an adsorption energy of −0.9 eV, large by physisorption standards but smaller than that obtained with the conventional zeolite Brønsted acid site. The N−H and O−H bond lengths of these structures are presented in Table 3. The large distance (1.48 Å) between framework oxygen (O_f) and H at the Si−OH−Al site after NH₃ adsorption further confirms the ion-pair formation.

Adsorption of BF₃ was found to be more favorable at the Si−NH−Si site than at the pristine sodalite Si−O−Si site, with adsorption energies of −0.8 and −0.5 eV, respectively, as shown in Table 4. This implies that sodalite becomes a much
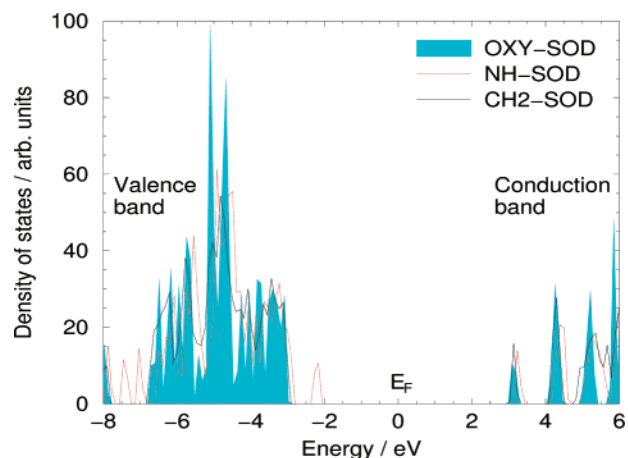
stronger Lewis base when amine-doped. The N−B distance in ≡Si−NH−Si≡−BF₃ indicates weak bonding involving the donation of N lone-pair electrons into BF₃ orbitals, while in OXY-SOD the corresponding distance is somewhat larger (Table 3).

The stabilization of nitrogen lone-pair electrons upon adsorption of BF₃ is also reflected in the electronic band structure of the system. The densities of the Kohn−Sham eigenstates of the pristine sodalite and the NH- and CH₂-doped sodalites containing one impurity are shown in Figure 4. No significant electronic activity, such as mid-gap states, is present in the pristine or CH₂-doped sodalites. However, the NH-doped sodalite exhibits a doubly occupied state 0.7 eV above the valence band edge. Upon BF₃ adsorption in the NH-doped sodalite, the energy of this state decreases to a value of 0.1 eV above the valence band edge. While one has to be careful not to confuse Kohn−Sham eigenenergies with physical one-electron energies, these band structure results clearly suggest that the NH impurity is an electron donor.

4. Concluding Remarks

We have computed structural properties of CH₂- and NH-doped sodalites, as well as CH₂-doped LTA zeolite, using plane-wave pseudopotential DFT-LDA methods. The purpose of this study is to investigate the mechanical stability of doped zeolites, and to examine whether impurities modify the chemical properties of zeolites in useful ways.

We found that Si−C−Si and Si−N−Si angles prefer to have substantially smaller values than the Si−O−Si angle in the pristine structures, while the more floppy Si−O−Si angles in the surrounding crystal take up the strain. Thus, a broad range of Si−O−Si angles is observed. In the CH₂-doped sodalites, the strain is also relieved by the contraction of the supercell, while in the NH doped sodalites, the volume change is less significant. At low defect concentrations, the strain contribution to the defect energy is estimated to be small, 0−0.15 eV, and a small increase is observed when the number of impurities increases from 2 to 3 (Figure 3). These strain energies were computed by comparing zeolite energies with energies of polymer reference systems. In the half- and fully doped structures, the defect strain energies have larger values, implying a threshold concentration at which there are not enough Si−

(30) Kapstin, G. I.; Brueva, T. R.; Mishin, I. V. In *Proceedings of the 12th International Zeolite Conference*; Treacey, M. M. J., Marcus, B. K., Bisher, M. E., Higgins, J. B., Eds.; Materials Research Society: Warrendale, PA, 1999; p 2637.

O−Si triplets to relieve the strain. The stability of defects is further supported by the observation that the Kohn−Sham eigenenergy band gap remains close to the pristine sodalite value and no strong electronic activity in the band gap region is detected.

Adsorption energies for various acid−base pairs in NH-doped and undoped sodalites were calculated. These values can be used to estimate the Brønsted acid and Lewis base strengths of the doped system. Sodalite containing Si−OH−Al was found to be a stronger acid than that containing Si−NH$_2$−Al, while Si−NH−Si was found to be a much stronger Lewis base than Si−O−Si. This electron donor property of the NH impurity is further supported by the behavior of the Kohn−Sham eigenstates. The enhanced Lewis base strength of NH doped sodalite suggests that such materials may be useful in base-catalysis applications such as partial oxidation[26] or halogen elimination.[27]

Although we should expect the acidity of amine-doped aluminosilicates to be weaker than that of conventional zeolites because oxygen's electronegativity exceeds that of nitrogen, the amine-doped systems offer chemical versatility lacking in the oxide acid. In particular, we imagine reactions such as:

$$\equiv Si-NXH-Al\equiv \; + \; NH_3(g) \rightleftharpoons$$
$$[\equiv Si-NX-Al\equiv]^{-1} + NH_4^{+}(ads)$$
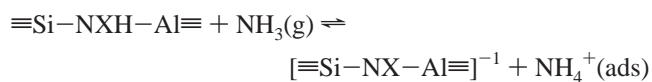
where the moiety X can be varied to tune acid strength to a desired level. For example, setting X = fluorine may increase the acidity; this is explored in a forthcoming publication.

Our results show that doping zeolites can produce minimal strain, even at high dopant concentrations. Furthermore, we have shown that doping can modify the zeolite's chemical properties in very interesting ways. Further computational studies can help to guide synthetic chemists as they try to design and fabricate new materials with advanced performance. Such computations might include studies of the kinetics of Si−N bond cleavage under synthesis conditions, to explore whether such linkages are likely to persist for long enough time scales.